Macromolecules
ARTICLE

Macromolecules **2011**, *44*, 1203–1210 **1203**
DOI: 10.1021/ma102658e

SANS Studies on Tetra-PEG Gel under Uniaxial Deformation

Takuro Matsunaga,[†] Hanako Asai,[†] Yuki Akagi,[‡] Takamasa Sakai,[‡] Ung-il Chung,[‡] and Mitsuhiro Shibayama*,[†]

[†]*Institute for Solid State Physics, The University of Tokyo, 5-1-5 Kashiwanoha, Kashiwa, Chiba 277-8581, Japan, and* [‡]*Department of Bioengineering, School of Engineering, The University of Tokyo, 7-3-1 Hongo, Bunkyo-ku, Tokyo 113-8656, Japan*

Received November 22, 2010; Revised Manuscript Received January 11, 2011

ABSTRACT: Studies on the deformation mechanism of polymer networks with small-angle neutron scattering (SANS) were carried out for Tetra-PEG gels, that is, poly(ethylene glycol) (PEG) networks prepared from tetra-functional A- and B-type macromers consisting of PEG by cross-end-coupling. Tetra-PEG gels are hydrogels with narrow-dispersed polymer chains. The molecular weights of the prepolymers were 20k and 40k. SANS measurements were conducted for uniaxially stretched Tetra-PEG gels. Although the SANS patterns for deformed Tetra-PEG gel-20k showed small anisotropy, that is, prolate and oblate patterns with respect to the stretching direction at low and high-q regions, respectively, Tetra-PEG gel-40k exhibited no anisotropy at all in the low-q region, even in a gel stretched by five times. This indicates that Tetra-PEG gel-40k is a homogeneous network free from inhomogeneities, such as dangling chains and entanglements and can be regarded as an "ideal" polymer network. The deformation mechanism of Tetra-PEG gels was discussed in comparison with those for phantom Gaussian chain model and others, suggesting that the concentration fluctuations by thermal motions surpass the chain anisotropy introduced by deformation.

Introduction

Elucidation of the deformation mechanism of polymer networks and polymer gels has been one of the most intriguing problems in polymer science for a number of decades.[1−7] The framework of rubber elasticity was constructed on the basis of randomly cross-linked Gaussian chain networks. There are a number of theories and models to describe the deformation of polymer networks, such as affine network model,[3,8] junction−affine network model,[9] phantom network model,[1,2,10] slip−link model,[11] and tube model.[12,13] Pioneering works on the phantom chain model by James and Guth in 1940s[1,2] and the scattering function for phantom chains proposed by Pearson[10] have been examined by a large number of investigators. Extensive discussions on the deformation mechanism of polymer networks were given by Flory in 1976.[5] Small-angle neutron scattering (SANS) is recognized to be one of the most suitable means to elucidate the relationship between the microscopic and macroscopic behaviors of deformation because polymer chains in a polymer network can be selectively labeled, and the change of polymer conformation can be studied as a function of macroscopic deformation.[14,15] Benoit et al. performed a pioneering work on the deformation of polymer network with SANS.[9] They performed SANS experiments on branch-labeled and labeled-chain networks of polystyrene. The former gave the information of the intercross-link distance, and the latter did the radius of gyration of labeled chains. They reported that both the change of the intercross-link distance and that of the radius of gyration were far below than those predicted by affine or junction-affine models. In the 1980s, a number of SANS investigations were carried out on deformed polymer networks. Ullman proposed scattering functions from labeled chains in polymeric networks for swollen and stretched polymer networks and compared them with those obtained by SANS experiments.[16−18] One of the important findings was that the chain deformation was less than that calculated from the phantom network model. Beltzung and coworkers reported the behavior of dry poly(dimethylsiloxane) networks submitted to uniaxial extension.[14] Boue et al. discussed the structure and dynamics of polymer networks under deformation.[15] These authors also concluded that knowledge of the chain deformation on the level of the mesh size of the network failed to provide all of the necessary information to correlate precisely the molecular processes with the macroscopic response of the network samples.

These examples clearly indicated that quantitative discussions on the deformation of polymer networks had not been available because of the lack of "ideal" polymer network suitable for quantitative comparison of polymer chain deformation between the theories and experiments. Here the "ideal" network means a polymer network consisting of monodisperse polymer chains without any defects, such as loops, dangling chains, and trapped entanglements. Recently, we developed near-"ideal" polymer networks called Tetra-PEG gels with negligible fractions of dangling chains and entanglements.[19−22] Here we report a series of SANS results on deformed Tetra-PEG gels and discuss the deformation mechanism. Focuses are placed on (1) the relationship of spatial inhomogeneities and the gel structure and (2) deformation mechanism of Tetra-PEG gels.

Theoretical Background

1. Deformation Models of Polymer Networks. If a polymer network is partially labeled with deuterated polymer chains, then the change of the radius of gyration of the labeled chains, R_g, is given as a function of the macroscopic deformation ratio, λ. There are several deformation models for

*To whom correspondence should be addressed.

Published on Web 02/01/2011

polymer networks, as introduced in the Introduction. Depending on the theories, the relationship between macroscopic and microscopic deformation is different as follows

(i) affine network model:

$$\frac{R_{g,\,para}}{R_{g,\,0}} \equiv \alpha_{aff,\,para} = \lambda, \frac{R_{g,\,perp}}{R_{g,\,0}} \equiv \alpha_{aff,\,perp} = \lambda^{-1/2} \quad (1)$$

where $R_{g.0}$ is the radius of gyration of the labeled chains in undeformed state. $R_{g,para}$ and $R_{g,perp}$ are those in the parallel and perpendicular directions in deformed state, respectively. However, in reality, the microscopic deformation of polymer network is different from that in macroscopic deformation because of thermal motions of polymer chains and other reasons. Well-known deformation models are junction−affine and phantom models.

(ii) junction−affine network model:

$$\frac{R_{g,\,para}}{R_{g,\,0}} \equiv \alpha_{j-aff,\,para} = \left(\frac{1+\lambda^2}{2}\right)^{1/2}$$

$$\frac{R_{g,\,perp}}{R_{g,\,0}} \equiv \alpha_{j-aff,\,perp} = \left(\frac{1+\lambda}{2\lambda}\right)^{1/2} \quad (2)$$

(iii) phantom network model:[10]

$$\frac{R_{g,\,para}}{R_{g,\,0}} = \alpha_{ph,para} = \left(\frac{f+2+(f-2)\lambda^2}{2f}\right)^{1/2} \quad (3a)$$

$$\frac{R_{g,\,perp}}{R_{g,\,0}} = \alpha_{ph,perp} = \left(\frac{f+2+(f-2)\lambda^{-1}}{2f}\right)^{1/2} \quad (3b)$$

Here f is the functionality of the cross-links. Evaluation of the ratio of the radius of gyrations after to before deformation allows one, in principle, to discuss the deformation mechanism of polymer networks.

2. SANS Functions for "Ideal" Polymer Networks. According to the de Gennes's C^* theorem, the scattering function for polymer gels is the same as that of the corresponding semidilute polymer solutions. Hence, by taking into account an excess scattering from gel inhomogeneities, $A_{ex}(q)$, the scattering intensity from a gel, $I(q)$, is given by[23]

$$I(q) = \frac{(\Delta\rho)^2 RT\phi^2}{N_A M_{os}}\left[\frac{1}{1+\xi^2 q^2} + A_{ex}(q)\right] \quad (4)$$

where N_A is the Avogadro's number, $\Delta\rho$ is the scattering density difference, R is the gas constant, T is the absolute temperature, ϕ is the polymer volume fraction, M_{OS} is the longitudinal modulus, and q is the magnitude of the scattering vector. ξ is the correlation length. $A_{ex}(q)$ is the excess scattering intensity dependent on the structure of inhomogeneities in the gel.[24] When $A_{ex}(q) = 0$, eq 4 is nothing but the so-called Ornstein−Zernike (OZ) function. The characteristic size of polymer network is given by the "blob" with size of ξ. When a gel is deformed, the blob is expected to be deformed to an ellipsoid with their principal axes to be ξ_{para} and ξ_{perp} in the direction of parallel and perpendicular directions, respectively. If the polymer network is fully labeled, for example, hydrogeneous polymer network in deuterated solvent, then deformation of the polymer network is observed as a deformation of blobs.[25,26] Hence

$$\xi_{para} = \alpha_{para}\xi_0, \xi_{perp} = \alpha_{perp}\xi_0 \quad (5)$$

By SANS experiments for deformed polymer networks, one would expect the microscopic deformation ratios, α_{para} and α_{perp} as a function of macroscopic deformation ratios, λ.

Experimental Section

Sample Preparation. Tetra-amine-terminated PEG (TAPEG) and tetra-NHS-glutarate-terminated PEG (TNPEG) were prepared from tetrahydroxyl-terminated PEG (THPEG) having equal arm lengths. Here NHS represents *N*-hydroxysuccinimide. The details of TAPEG and TNPEG preparation are reported elsewhere.[19] Equal amounts of TAPEG and TNPEG were dissolved in phosphate buffer (pH 7.4) and phosphate-citric acid buffer (pH 5.8), respectively, and the resulting solution was poured in the mold with the size of 60 mm long × 45 mm wide × 3 mm thick. Note that buffer solutions were prepared with deuterated water to reduce the incoherent scattering from H-containing materials. To control the reaction rate, we chose the ionic strengths of the buffers to be 100 mM. At least 12 h were spent for the completion of the reaction before the following experiments. The molecular weights (M_w) of TAPEG and TNPEG were matched to each other, and two sets of macromers having different M_w values were prepared, that is, M_w = 20k and 40k g/mol. The sample code is given by the M_w, for example, Tetra-PEG gel-20k being Tetra-PEG with $M_w = 20 \times 10^3$ g/mol. Constant amounts of TAPEG and TNPEG (M_w = 20k g/mol, 100 mg/mL and M_w = 40k g/mol, 140 mg/mL) were dissolved in phosphate-buffered D_2O (pH 7.4) and phosphate-citric-acid-buffered D_2O (pH 5.8), respectively. The specimens were used in as-prepared state.

Stretching Measurement. The stretching measurement was carried out on dumb-bell-shaped films using a mechanical testing apparatus (CR-500DX-SII rheometer; Sun Scientific, Tokyo, Japan) at a crosshead speed of 0.1 mm/sec. The sample thickness for the stretching measurement was 1 mm.

Small-Angle Neutron Scattering. SANS experiments were performed at the 2D SANS instrument (SANS-U), Neutron Science Laboratory, University of Tokyo.[27,28] The neutron wavelength was 7.0 Å. The monochromatization was attained with a mechanical velocity selector, and the wavelength distribution was ca. 10%. The sample-to-detector distances (SDDs) were 2 and 8 m, which cover the q range of 0.005 to 0.2 $Å^{-1}$. The scattered neutrons were collected with a 2D detector (model 2660N, Ordela).

Deformation SANS experiments were carried out for reed-shaped samples held on a stretching device equipped in a laboratory-made stretching chamber. The initial cross-head distance was 20 mm. Although there is a possibility of a biaxial deformation, we employed the reed-shaped specimens under the limitation of experimental conditions, such as the limitation of sample size, the space of SANS sample stage (smaller is better), and the necessary neutron beam size (larger is better). The humidity of the sample environment was kept constant by placing a bottle of water near the sample in a shielded-stretching chamber throughout the experiment. After a gel sample was loaded, the humidity and temperature were equilibrated within 5 min. The stretching was driven by a stepping motor. The stretching rate was 70 mm/min. Whenever the samples were stretched, SANS experiments were started after waiting for 10 min. The observed scattered intensity functions were corrected for air scattering, incoherent scattering, and transmission and then were rescaled to the absolute intensity, $I(q)$, with a polyethylene secondary standard. Incoherent scattering intensity subtraction was made with the T-method reported elsewhere.[29]

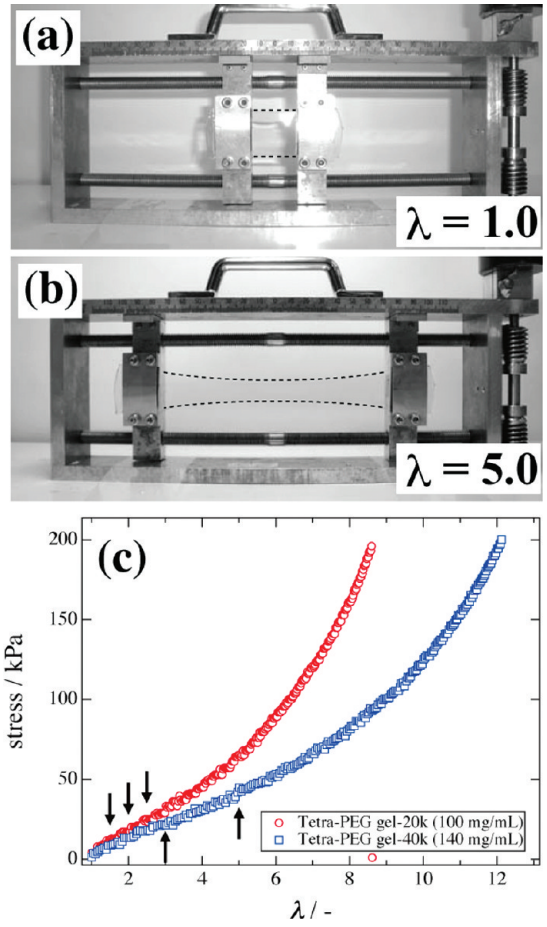

Figure 1. Photographs of Tetra-PEG gel-40k in (a) nonstretched state ($\lambda = 1.0$) and (b) stretched state ($\lambda = 5.0$). (c) Stretching stress−strain curves of Tetra-PEG gel-20k and -40k. The stretching ratios at which SANS experiments were carried out are marked by arrows.

Results and Discussion

1. Stress−Elongation Curves of Tetra-PEG Gels. First of all, let us show the stress−elongation curves of Tetra-PEG gel-20k and -40k before beginning to discuss the SANS results, where λ is the stretching ratio. Figure 1a,b shows the photographs of Tetra-PEG gel-40k at $\lambda = 1.0$ and 5.0 on the laboratory-made stretching device for SANS experiments. As shown in Figure 1b, Tetra-PEG gels can be deformed like a stripe of rubber. Figure 1c shows the stretching stress−elongation curves of Tetra-PEG gel-20k (100 mg/mL) and -40k (140 mg/mL). These concentrations were the same as those in the SANS experiments. The stretching ratios at which SANS measurements were carried out are marked by arrows in the Figure ($\lambda = 1.0$, 1.5, 2.0, 2.5, 3.0, and 5.0). The stretching ratios of $\lambda = 2.5$ for Tetra-PEG gel-20k and $\lambda = 5.0$ for Tetra-PEG gel-40k are close to the crossover from Gaussian to Non-Gaussian region. Therefore, the molecular chains in the network were stretched large enough.

2. Tetra-PEG Gel-20k. Figure 2 shows 2D-SANS scattering patterns obtained for uniaxially deformed Tetra-PEG gel-20k (100 mg/mL). The stretching ratios were $\lambda = 1.0$, 1.5, 2.0, and 2.5. The stretching direction was horizontal. The upper and lower figures show SANS patterns taken at SDD = 8 and 2 m, respectively. As shown in the Figure, both scattering patterns (SDD = 8 and 2 m) had isotropic patterns at $\lambda = 1.0$. When the samples were stretched, anisotropic patterns appeared in both low-q (8 m SANS data) and high-q regions (2 m SANS data). Note that the 8 m SANS patterns showed a two-lobe pattern in the stretching direction at $\lambda = 2.0$ and 2.5 (the so-called abnormal butterfly pattern). The 2 m SANS patterns became slightly elliptic with their long axis perpendicular to the stretching direction (the so-called a normal butterfly pattern). It is noteworthy that marked anisotropic patterns (called "abnormal butterfly patterns") are commonly observed in polymer gels because of spatial inhomogeneities, even with the elongation ratio of less than $\lambda = 2$.[26,30−32] Therefore, the result shown in Figure 2 is rather surprising. In the case of Tetra-PEG gels, furthermore, no inhomogeneities were observed, even in swollen gels, as discussed in our previous paper.[23] Hence, this is the first time to observe anisotropic inhomogeneities in a Tetra-PEG gel network.

Figure 3 shows the sector-averaged scattering intensities in the parallel and perpendicular directions for Tetra-PEG gel-20k (Figure 2). Here the sector average was taken with the sector angle of ±10° with respect to the parallel and perpendicular directions. The SANS curve for unstretched sample (circles) was obtained by taking circular averaging; the dashed line indicates a theoretical fit with eq 4 by setting $A_{ex}(q) = 0$, and the obtained ξ value was 13 Å. As shown here, there is a clear difference in the low-q region, that is, an upturn in the intensity for $q \leq 0.02$ Å^{-1} in the parallel direction (△) and a suppression in the perpendicular direction (▲). A different type of anisotropy was observed in the high-q region ($q \geq 0.04$ Å^{-1}), that is, an elliptic pattern in the perpendicular direction. Because this q region corresponds to the thermal fluctuations of polymer chains in a blob, it is deduced that polymer chains are somewhat stretched in the stretching direction.

To characterize the anisotropy in the SANS patterns, we calculated annular averages for two different q values. Figure 4 shows an azimuthal−angle plot of the scattering intensities at $q = 0.010$ ($0.0084 < q < 0.012$ Å^{-1}) and 0.072 Å^{-1} ($0.054 < q < 0.089$ Å^{-1}) with various stretching ratios. ψ is the azimuthal angle on the 2D detector plane, and $\psi = 0$ is defined as the stretching direction. The azimuthal angle was taken with an interval of 10°. $q = 0.010$ and 0.072 Å^{-1} correspond to representative anisotropic regions of the low- and high-q, respectively. It is needless to mention that the unstretched sample gives a ψ-independent pattern. As shown in the Figure, both q regions show ψ dependence by increasing stretching ratio. Note that there is a phase difference by 90°. This means that the anisotropy directions of low- and high-q are opposite. We employed the following Gaussian equations for the curve fitting.

$$I(\psi) = A\sum_{i=0}^{2}\exp\left\{-\frac{(\psi - 180i)^2}{2\sigma^2}\right\} + B \quad \text{(low-}q\text{)} \qquad (6)$$

$$I(\psi) = A\sum_{i=1}^{2}\exp\left\{-\frac{(\psi - 90(2i-1))^2}{2\sigma^2}\right\} + B \quad \text{(high-}q\text{)} \qquad (7)$$

where A is the amplitude (height) of the modulation, σ^2 is the variance, and B is the baseline. Here the full width at half-maximum (fwhm) of Gaussian is defined by fwhm = $2(2\ln 2\sigma)^{1/2}$. In the case of strong anisotropy, A and fwhm become larger and smaller, respectively. Here we define the degree of anisotropy with the ratio of A/fwhm and discuss it as a function of the stretching. Note that parallel and perpendicular orientations are indicated by positive and negative signs, respectively. Figure 5 shows the degree of anisotropies at the different scattering intensities $I(q = 0.010$ Å$^{-1})$

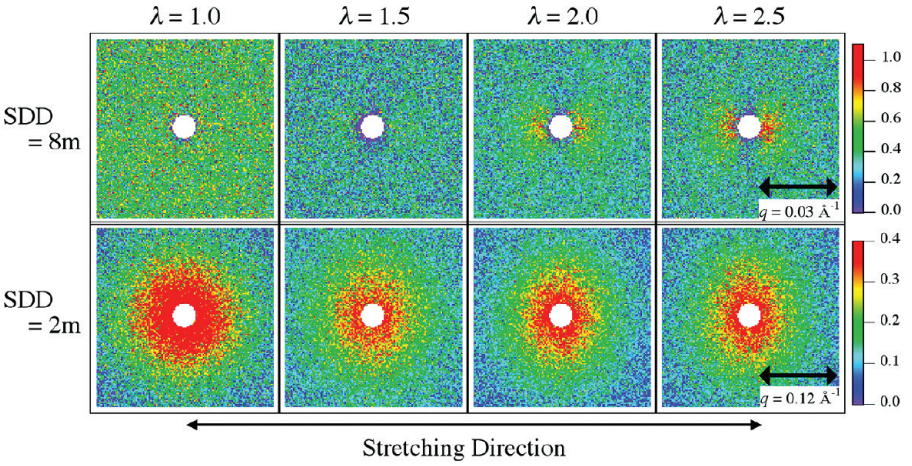

Figure 2. Two-dimensional SANS patterns of Tetra-PEG gel-20k (100 mg/mL) at SDD = 8 (top) and 2 m (bottom). Stretching ratios are λ = 1.0, 1.5, 2.0, and 2.5.

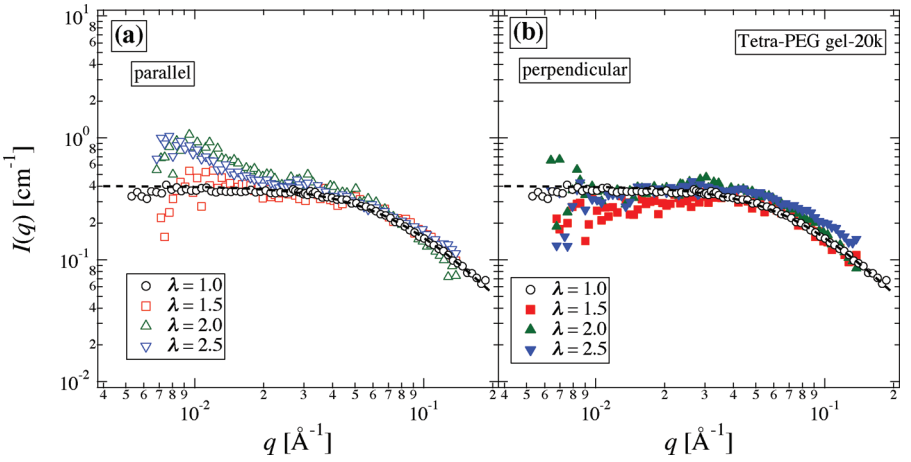

Figure 3. Sector-averaged scattering intensities (±10°) for Tetra-PEG gel-20k at different stretching ratios (a) parallel and (b) perpendicular direction to the stretching direction. The dashed line indicates the curve fit with OZ function.

and $I(q = 0.072\ \text{Å}^{-1})$. It is clearly shown that the degree of anisotropy increased with increasing stretching ratio, λ, and the anisotropies in the low-q (inhomogeneities; defects) and high-q (blob; polymer chains) regions behave oppositely.

3. Nonstoichiometric Tetra-PEG Gel-20k. In the case of Tetra-PEG gels, it is of particular importance to match the concentration of TAPEG and TNPEG for obtaining defect-free polymer networks and achieving optimal mechanical properties.[21] If a stoichiometric condition is broken, then the mechanical properties drastically deteriorate as reported elsewhere.[21] To investigate the effect of defects (dangling chains) in polymer networks under deformation, we intentionally introduced dangling chains by preparing nonstoichiometric Tetra-PEG gels with the following compositions; [TAPEG]:[TNPEG] 1.1:0.9, 1.2:0.8, and 1.3:0.7. Figure 6 shows the azimuthal plots of scattering intensities for non-stoichiometric 100 mg/mL Tetra-PEG gel-20k. All samples were measured at λ = 2.0. As shown in the Figure, anisotropic scattering patterns were obtained at all compositions similar to the case of the stoichiometric gel ([TAPEG]:[TNPEG] 1.0:1.0). Figure 7 shows the degree of anisotropy obtained from the curve fitting with eqs 6 and 7 for non-stoichiometric Tetra-PEG gels. We expected that the degree of anisotropy would increase for the low-q region because of an introduction of defects. This is because inhomogeneities are known to be amplified by deformation, such as stretching or swelling.[30,33] Interestingly, however, the degrees of anisotropy of both of the two ranges were suppressed with increasing asymmetry in the composition. The reasons why the degree of anisotropy decreased are explained as follows. By introducing defects (i.e., dangling chains), deformation is localized around the defect regions, and perfect network regions become less deformed by stretching with the cost of a larger deformation of the defect regions. As a result, the anisotropy of high-q region (i.e., blob deformation) becomes small. Similarly, the anisotropy of low-q region is also suppressed because of the same reason at the high-q region, despite the number of defects increases. Note that such decrease in the degree of anisotropy by introducing defects may apply only to near-"ideal" network like Tetra-PEG gels.[22] Strong inhomogeneities observed in the literature[24] may be ascribed to densely cross-linked zones in a network. That is, conventional gels having a large fraction of various types of defects, such as dangling chains, trapped entanglements, and loops, would show an increase in anisotropy when deformed by further introducing defects.

4. Tetra-PEG Gel-40k. Figure 8 shows the SANS 2D patterns for Tetra-PEG gel-40k (140 mg/mL) under uniaxial deformation. The stretching ratios were λ = 1.0, 3.0, and 5.0. At SDD = 2 m, the scattering patterns at λ = 1.0 were isotropic. However, to our surprise, anisotropy in the SANS patterns for deformed gels is hard to recognize. A careful

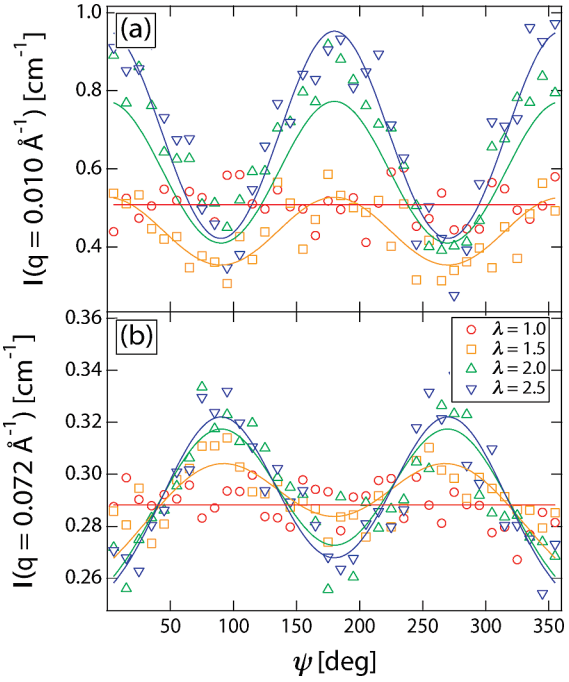

Figure 4. Azimuthal plots of SANS intensities for Tetra-PEG gel-20k at (a) $q = 0.010$ Å^{-1} and (b) $q = 0.072$ Å^{-1}. $\lambda = 2.0$.

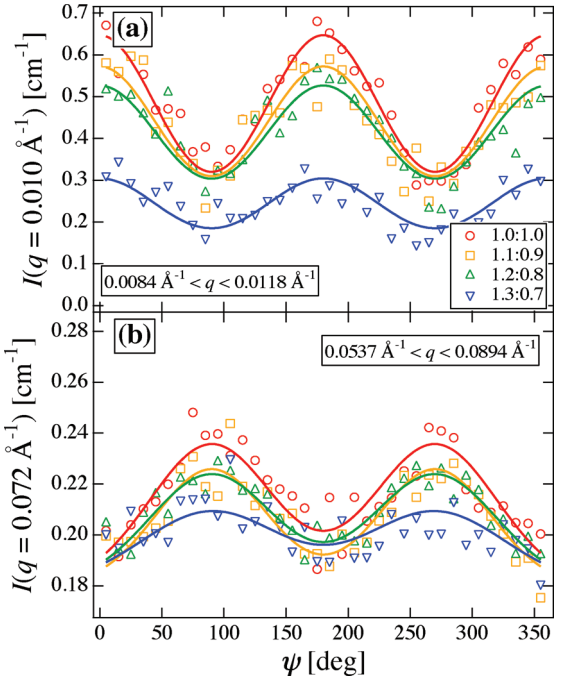

Figure 6. Azimuthal plots of SANS for nonstoichiometric gels at (a) $q = 0.010$ Å^{-1} and (b) $q = 0.072$ Å^{-1}. $\lambda = 2.0$.

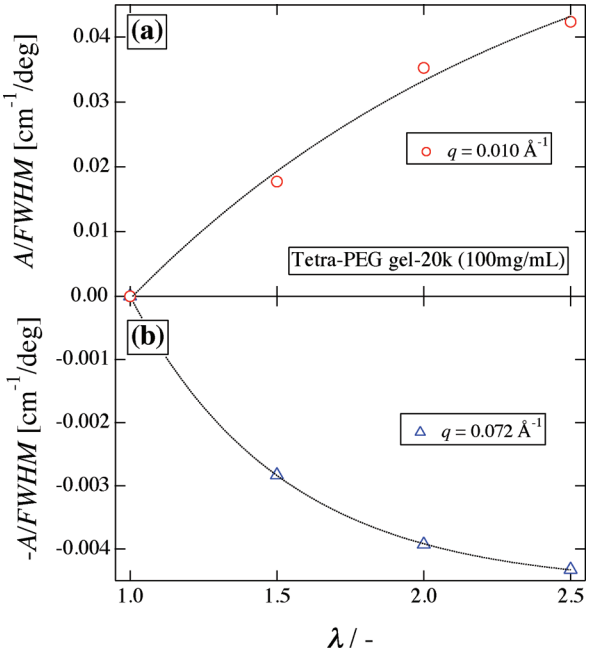

Figure 5. Degree of anisotropy at low- and high-q regions for Tetra-PEG gel-20k evaluated with eqs 6 and 7. The dotted lines are for the eye.

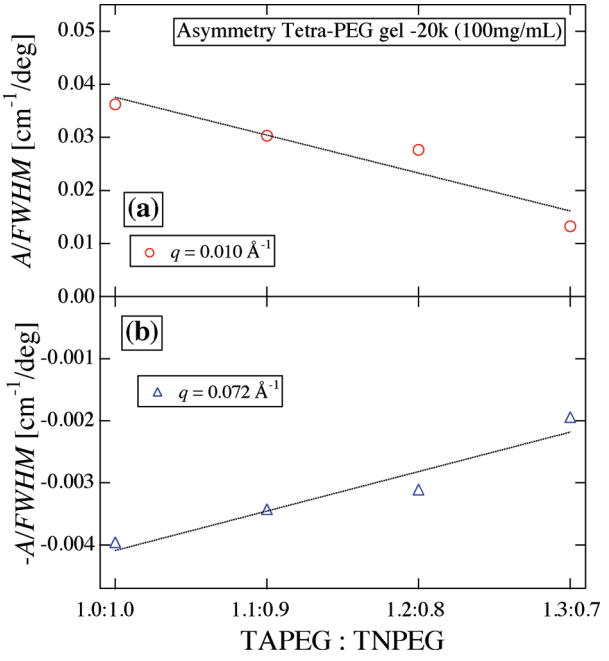

Figure 7. Degree of anisotropy at low- and high-q regions for non-stoichiometric Tetra-PEG gel-20k evaluated with eqs 6 and 7. The dotted lines are for the eye.

observation leads us to acknowledge that the scattering patterns at SDD = 8 m differ substantially from that of Tetra-PEG gel-20k. (See Figure 2.) No anisotropy was detected at all at stretching ratios up to $\lambda = 5.0$, at least in the low-q region ($0.005 \leq q \leq 0.05$ Å^{-1}).

Figure 9 shows the sector-averaged scattering intensities in the parallel and perpendicular directions to the stretching direction for Figure 8. Here the sector average was taken similarly to the case of Tetra-PEG gel-20k. It should be noted that no noticeable inhomogeneities were observed in deformed gel at the low-q region ($q = 0.010$ Å^{-1}). Because we reported in the previous paper that Tetra-PEG gel-40k is closer to an ideal network than other Tetra-PEG gels with lower M_W values based on the results of the swelling and SANS experiments,[23] it can be concluded that Tetra-PEG gel-40k forms a very homogeneous network. The SANS functions can be fitted with eq 4 (again with $A_{ex}(q) = 0$) with $\xi = 9.0$ Å. This value is on the order of the monomer segment length of PEG. This means that the concentration fluctuations in Tetra-PEG gel-40k are of the order of monomer.

To elucidate the anisotropy of thermal fluctuation at high-q region, we obtained an azimuthal plot for Tetra-PEG

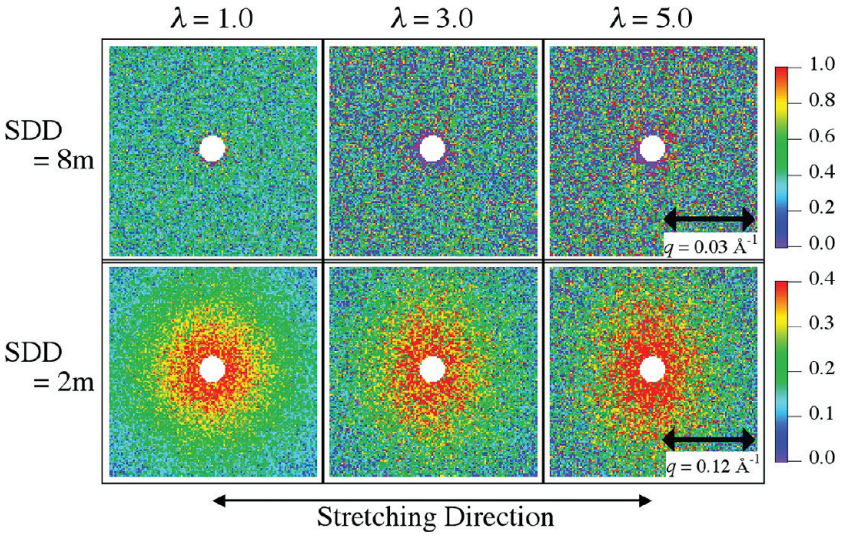

Figure 8. SANS 2D patterns for Tetra-PEG gel-40k at SDD = 8 (top) and 2 m (bottom). Stretching ratios are λ = 1.0, 3.0, and 5.0.

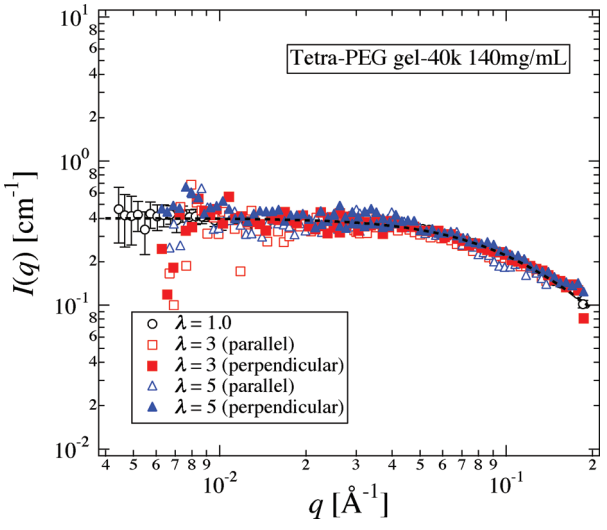

Figure 9. Sector-averaged scattering intensities (±10°) for Tetra-PEG gel-40k at different stretching ratios. The dashed line indicates the curve fit with OZ function.

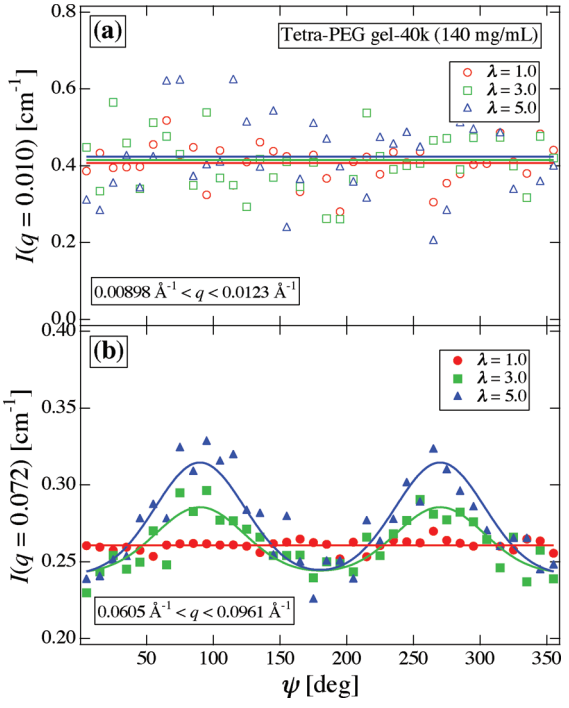

Figure 10. Azimuthal plots of SANS intensities for Tetra-PEG gel-40k at (a) q = 0.010 Å^{-1} and (b) q = 0.072 Å^{-1}. λ = 2.0.

gel-40k. Figure 10 shows the result. It is clear from the Figure that the anisotropy of Tetra-PEG gel-40k was much less than that of Tetra-PEG gel-20k (Figure 4). Figure 11 shows the variation of the degree of anisotropies at low- and high-q. The degree of anisotropy at high-q was about a half of that of Tetra-PEG gel-20k when compared at the same value of λ.

5. Deformation Mechanism of Tetra-PEG Gels. In the literature, there are many discussions on the relationship between the macroscopic and microscopic deformation,[14−17] where the change of the radius of gyration, R_g, was plotted as a function of the macroscopic deformation ratio. However, the length parameter studied in polymer gels is, in most cases, the correlation length, which is a measure of the range of thermal concentration fluctuations. If the correlation length carries some information of network inhomogeneities, then it shows anisotropic change by stretching deformation, as studied by Geissler et al.,[34] Mendes et al.,[26,31] and by Shibayama et al.[32] When the deformation mechanism is discussed for polymer gels, the anisotropy in the correlation length is often plotted, similar to the case of R_g, as a function of the macroscopic deformation ratio by using the relationship of eq 5.[26,32] Figure 12 shows the plot of the microscopic deformation ratios, α_{para} and α_{perp}, as a function of macroscopic deformation ratio, λ. As shown here, the variation of the experimental values, that is, α_{para} and α_{perp}, for Tetra-PEG gels were negligibly small, and none of the polymer network models worked at all. Mendes et al. observed strong anisotropy in SANS functions, that is, abnormal butterfly pattern, for fully labeled networks and concluded that these patterns could not be explained by the classical theories of network deformation.[26] Then, they tried to fit the anisotropic SANS functions with those predicted by various theories, such as heterogeneous model,[25] thermal heterogeneous model by Onuki,[35] the strain−concentration coupling model by Rabin and Bruinsma.[36,37] However, the agreement was rather poor.

Now let us discuss the scientific significance of the experimental finding shown in Figure 12. In the case of Beltzung

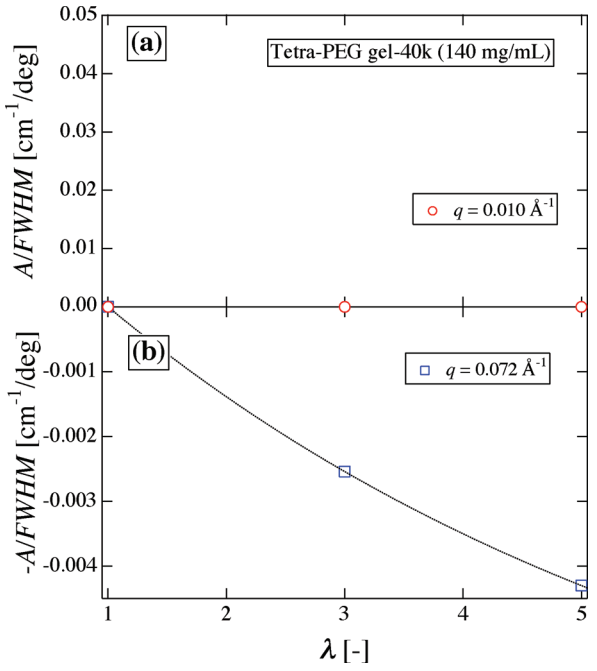

Figure 11. Degree of anisotropy at low- and high-q regions for Tetra-PEG gel-40k evaluated with eqs 6 and 7. The dotted lines are for the eye.

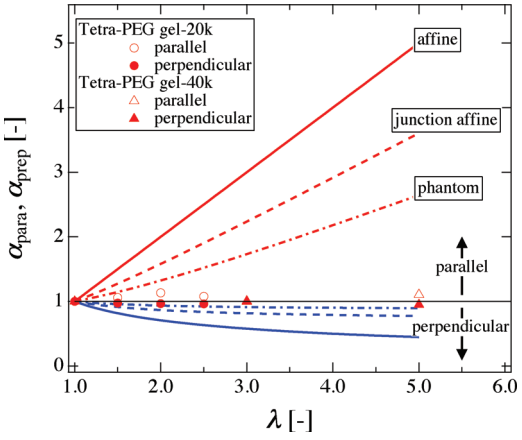

Figure 12. Variation of microscopic stretching ratios as a function of macroscopic stretching ratio, for affine (solid line), junction−affine (dashed line), phantom chain (chain line), and Tetra-PEG gels (circles and triangles).

and coworkers, the "phantom-like" behavior of the labeled chains in a network is ascribed not only to thermal motions of cross-links as well as the polymer chain segments but also to (i) imperfect cross-linking reaction and (ii) "constraint" of network chains, that is, a high population of spatial neighbor cross-links within a domain characterized by topological neighbor cross-links. Regarding (ii), it is meaningful to discuss the ratio of the spatial to topological neighbor cross-links, Γ, that is, the number of spatial neighbors per topological neighbors. Γ can be evaluated by[5,14]

$$\Gamma = \frac{4\pi}{3} n^{1/2} \text{ (for bulk polymer network)} \quad (8a)$$

$$\Gamma = \frac{4\pi}{3} \phi n^{4/5} \text{ (for swollen gel)} \quad (8b)$$

where n is the degree of polymerization between neighboring cross-links and ϕ is the polymer volume fraction. The value of Γ is on the order of a few tens to hundreds for bulk polymer networks whereas it is on the order of unity for highly swollen gels. Therefore, fluctuations of polymer chains in bulk network are strongly suppressed by spatial neighbors. The disagreement in the behavior of the correlation length between the theory and the experiments for fully labeled polymer networks must be mainly ascribed to the ill-formed networks with large inhomogeneities in these gels.

In the case of Tetra-PEG gels, it is reported that there are no entanglements in the blob defined by the topological neighbors.[20,22] Furthermore, the concentrations of Tetra-PEG gels employed in this work are rather high (e.g., 100 mg/mL for Tetra-PEG gel-20k and 140 mg/mL for Tetra-PEG gel-40k) to attain a large stretching ratio, for example, $\lambda = 5.0$. In this concentration range, the measure of concentration fluctuations (i.e., the correlation length) is 13 or 9.0 Å, which is much smaller than the radius of gyration of Tetra-PEG macromers (20.1 and 20.6 Å, respectively, for Tetra-PEG-20k (100 mg/mL) and Tetra-PEG-40k (140 mg/mL))[23] and very close to the monomer size. Hence, only thermal fluctuations around the neighborhood of the monomer itself may be possible. As a result, the concentration fluctuations observed as the correlation length is solely due to segmental thermal fluctuations in the solvent irrespective of the stretching ratio. This is a piece of strong evidence of "ideal" polymer network. Comparison of the mechanical properties between experiments and theories will be reported in the forthcoming paper.

Conclusions

The deformation mechanism of polymer networks was investigated by using "ideal" polymer network, Tetra-PEG gels. Tetra-PEG gel-20k showed a slight change in the scattering intensity by deformation. An upturn in the intensity was observed at low-q region, indicating the emergence of inhomogeneities. Tetra-PEG gel-40k did not show any anisotropy at low-q region ($0.005 \le q \le 0.05$ Å^{-1}). Although a very small anisotropy appeared by stretching the gel by five times, essentially no anisotropy was observed in Tetra-PEG gel-40k. Thermal concentration fluctuations were observed because of a segmental motion around its mean position irrespective of the stretching ratio. In any case, this is the first time, to our knowledge, that deformation mechanism of polymer networks is discussed with a well-defined polymer network, and no anisotropy is observed in SANS for largely deformed gel. The intentional introduction of dangling chains to polymer network resulted in lowering in network inhomogeneities. This was explained with the suppression of deformation of the majority of the network with the cost of local deformation of the defect regions.

Acknowledgment. This work was partially supported by the Ministry of Education, Science, Sports and Culture, Japan (Grant-in-Aid for Scientific Research (A), 2010-2012, no. 22245018, and for Scientific Research on Priority Areas, 2006-2010, no. 18068004)). The SANS experiment was performed with the approval of Institute for Solid State Physics, The University of Tokyo (proposal nos. 10621 and 10629), at Japan Atomic Energy Agency, Tokai, Japan. This work was carried out by the support of Atomic Energy Initiative, MEXT. T.M. acknowledges the support from Research Fellowship for Young Scientists of the Japan Society for the Promotion of Science.

References and Notes

(1) Guth, E.; James, H. M. *Rubber Chem. Technol.* **1941**, *14*, 596.
(2) James, H. M.; Guth, E. *J. Chem. Phys.* **1947**, *15*, 669–683.
(3) Flory, P. J.; Rehner, J., Jr. *J. Chem. Phys.* **1943**, *11*, 521–526.
(4) James, H. M.; Guth, E. *J. Chem. Phys.* **1953**, *21*, 1039–1049.

(5) Flory, P. J.; Gordon, M.; McCrum, N. G. *Proc. R. Soc. London, Ser. A* **1976**, *351*, 351–380.
(6) Treloar, L. R. G. *The Physics of Rubber Elasticity*; Clarendon Press: Oxford, U.K., 1975.
(7) Mark, J. E.; Erman, B. *Rubberlike Elasticity: A Molecular Primer*; Wiley: New York, 1988.
(8) Flory, P. J. *Principles of Polymer Chemistry*; Cornell University: Ithaca, NY, 1953.
(9) Benoit, H.; Decker, D.; Duplessix, C.; Picot, C.; Rempp, P. *J. Polym. Sci., Polym. Phys. Ed.* **1976**, *14*, 2199–2128.
(10) Pearson, D. S. *Macromolecules* **1977**, *10*, 696–701.
(11) Ball, R. C.; Edwards, S. F.; Doi, M.; Warner, M. *Polymer* **1981**, *22*, 1010–1018.
(12) Doi, M.; Edwards, S. F. *The Theory of Polymer Dynamics*; Oxford University Press: Oxford, U.K., 1986.
(13) Gaylord, R. J. *Polym. Bull.* **1982**, *8*, 325–329.
(14) Beltzung, M.; Picot, C.; Herz, J. *Macromolecules* **1984**, *17*, 663–669.
(15) Boue, F.; Bastide, J.; Buzier, M., SANS Probing of Statics and Dynamics of Polymer Networks Under Deformation: Relation Between the Scatterings of Labeled Paths and Labeled Free Chains Dissolved in the Network. In *Molecular Basis of Polymer Networks*; Baumgartner, A., Picot, C. E., Eds.; Springer: Berlin, 1989; pp 65−81.
(16) Ullman, R. *Macromolecules* **1982**, *15*, 582–588.
(17) Ullman, R. *Macromolecules* **1982**, *15*, 1395–1402.
(18) Tsay, H. M.; Ullman, R. *Macromolecules* **1988**, *21*, 2963–2972.
(19) Sakai, T.; Matsunaga, T.; Yamamoto, Y.; Ito, C.; Yoshida, R.; Suzuki, S.; Sasaki, N.; Shibayama, M.; Chung, U. *Macromoleules* **2008**, *41*, 5379–5384.
(20) Akagi, Y.; Matsunaga, T.; Shibayama, M.; Chung, U.; Sakai, T. *Macromolecules* **2010**, *43*, 488–493.
(21) Matsunaga, T.; Sakai, T.; Akagi, Y.; Chung, U.; Shibayama, M. *Macromolecules* **2009**, *42*, 1344–1351.
(22) Sakai, T.; Matsunaga, T.; Akagi, Y.; Kurakazu, M.; Chung, U.; Shibayama, M. *Macromol. Rapid Commun.* **2010**, *31*, 1954–1959.
(23) Matsunaga, T.; Sakai, T.; Akagi, Y.; Chung, U.; Shibayama, M. *Macromolecules* **2009**, *42*, 6245–6252.
(24) Shibayama, M. *Macromol. Chem. Phys.* **1998**, *199*, 1–30.
(25) Bastide, J.; Leibler, L.; Prost, J. *Macromolecules* **1990**, *23*, 1821–1825.
(26) Mendes, E.; Oeser, R.; Hayes, C.; Boue, F.; Bastide, J. *Macromolecules* **1996**, *29*, 5574–5584.
(27) Okabe, S.; Nagao, M.; Karino, T.; Watanabe, S.; Adachi, T.; Shimizu, H.; Shibayama, M. *J. Appl. Crystallogr.* **2005**, *38*, 1035–1037.
(28) Okabe, S.; Karino, T.; Nagao, M.; Watanabe, S.; Shibayama, M. *Nuclear Instruments & Methods in Physics Research, Section A* **2007**, *572*, 853–858.
(29) Shibayama, M.; Matsunaga, T.; Nagao, M. *J. Appl. Crystallogr.* **2009**, *42*, 621–628.
(30) Mendes, E. J.; Lindner, P.; Buzier, M.; Boue, F.; Bastide, J. *Phys. Rev. Lett.* **1991**, *66*, 1595–1598.
(31) Mendes, E.; Schosseler, F.; Isel, F.; Boue, F.; Bastide, J.; Candau, S. J. *Europhys. Lett.* **1995**, *32*, 273–278.
(32) Shibayama, M.; Kawakubo, K.; Ikkai, F.; Imai, M. *Macromolecules* **1998**, *31*, 2586–2592.
(33) Bastide, J.; Leibler, L. *Macromolecules* **1988**, *21*, 2647–2649.
(34) Geissler, E.; Horkay, F.; Hecht, A. M. *J. Chem. Phys.* **1995**, *102*, 9129–9132.
(35) Onuki, A. *J. Phys. II* **1992**, *2*, 45–61.
(36) Rabin, Y.; Bruinsma, R. *Europhys. Lett.* **1992**, *20*, 79–85.
(37) Bruinsma, R.; Rabin, Y. *Phys. Rev. E* **1994**, *49*, 554–569.